EurJOC
European Journal of Organic Chemistry

A Journal of
ChemPubSoc Europe

Accepted Article

Title: Redox Center Modification of Lapachones Toward the Syntheses of Nitrogenated Heterocycles as Selective Fluorescent Mitochondrial Imaging Probes

Authors: Fabíola dos Santos, Gleiston G. Dias, Rossimiriam P. de Freitas, Lucas S. Santos, Guilherme F. de Lima, Hélio A. Duarte, Carlos A. de Simone, Lidia Rezende, Monique J. X. Vianna, José R. Correa, Brenno A. D. Neto, and Eufrânio Nunes da Silva Júnior

To be cited as: *Eur. J. Org. Chem.* 10.1002/ejoc.201700227

Link to VoR: http://dx.doi.org/10.1002/ejoc.201700227

Supported by
ACES Asian Chemical Editorial Society

WILEY-VCH

Redox Center Modification of Lapachones Toward the Syntheses of Nitrogenated Heterocycles as Selective Fluorescent Mitochondrial Imaging Probes

Fabíola S. dos Santos,[a]1 Gleiston G. Dias,[a]1 Rossimiriam P. de Freitas,[a] Lucas S. Santos,[a] Guilherme F. de Lima,[a] Hélio A. Duarte,[a] Carlos A. de Simone,[b] Lidia M. S. L. Rezende,[c] Monique J. X. Vianna,[c] José R. Correa,[c] Brenno A. D. Neto[c] and Eufrânio N. da Silva Júnior*[a]

Abstract: This work describes a synthetic strategy for the syntheses of new fluorescent imidazole and phenazine derivatives synthesized from lapachol, a naturally occurring naphthoquinone isolated from *Tabebuia* species (*ipê* tree). Photophysical properties and computational details of these compounds were studied aiming at a complete understanding of the potential of these derivatives as probes capable of staining mitochondria selectively. Cell imaging experiments proved the imidazole derivatives capacity as selective fluorescent mitochondrial imaging probes. These heterocycles presented the same staining patterns of MitoTracker red corroborating the potential of these compounds as new mitochondria markers permeable to the cell membrane.

Introduction

Inspiration from nature toward chemical transformations and new compounds syntheses is virtually unlimited.[1] Versatile synthons and intermediates may be directly accessed and, in many cases, multigram access is not a drawback for fine chemical transformations. β-Lapachone and its derivatives are among these classes of natural substrates widely used for a plethora of applications such as organic chemistry transformation,[2] anticancer agents,[3] trypanocidal[4] and many others.[5] Lapachol is a naturally occurring naphthoquinones[6] prone to several chemical modifications, attracting therefore, the interest for the possibilities of structural diversity and applications.[7]

The opportunity of generating heterocyclic compounds from naphthoquinoidal derivatives obtained from lapachones in a straight fashion is an additional feature to be considered (Scheme 1A).[8,9] For example, our group have recently demonstrated the application of this strategy for the synthesis of fluorescent oxazoles,[10] boron complexes mimic BODIPYs[11] and phenazine-based 1,2,3-triazole[12] (Scheme 1B). We have shown that the lipophilic oxazoles are able to use for selective cellular staining of lipid-based structures. In the same way, we have designed and prepared boron complexes of oxazole derivatives easily obtained from lapachol. These compounds were observed as superior and selective probes for endocytic pathway tracking in live cancer cells. Finally, phenazine-based 1,2,3-triazole was efficient for determining Cd^{2+} ions in H_2O/CH_3CN medium. Later, our group have also studied the indirect consequences of exciplex states on the phosphorescence lifetime of this phenazinic compound.[13] Taking into account the large number of possible substituents and also the easy π-conjugation (beneficial effect for fluorescence emissions) one may rationalize several new bioprobes from lapachones.

Fluorescent phenazines[14-16] and their complexes may be used to stain different cell organelles as well as fluorescent imidazoles.[17-19] Among the almost uncountable possibilities of specific staining inside live cells, the mitochondria are organelles of paramount importance.[20] Known to be the membrane-bound powerhouse of eukaryotic cells,[21] the dysfunction of this organelle is related to several diseases[22-24] or apoptotic processes.[25-27] The specific staining of mitochondria is even more challenge whether one consider that these organelles vary the size, morphology, dynamics and quantities from organism to organism.[28] To follow the mitochondrial dynamics in live cells is indeed a hard task[29] where fluorescent small molecule probes are key players toward the understanding and roles of many factors affecting the mitochondrial regular function.[30]

Due of our interest on the development of new and selective bioprobes,[31] especially for mitochondrial selective staining,[32-34] we disclose herein our synthetic strategy in the syntheses of new fluorescent imidazole and phenazine derivatives from lapachone toward selective mitochondrial staining in live cells.

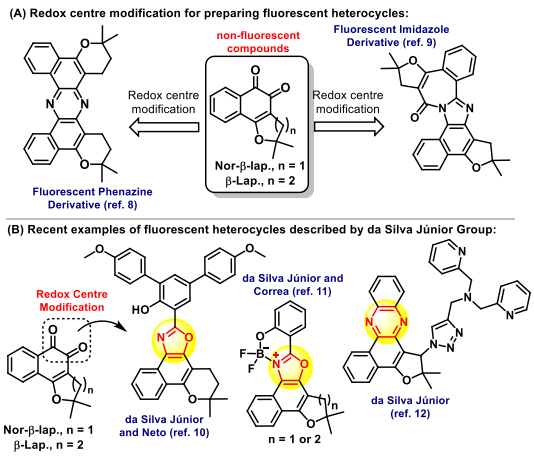

Scheme 1. Redox centre modification of lapachones to afford fluorescent imidazole, oxazoles and phenazine derivatives.

[a] Institute of Exact Sciences, Department of Chemistry, Federal University of Minas Gerais, Belo Horizonte, 31270-901, MG, Brazil. E-mail: eufranio@ufmg.br
[b] Department of Physics and Informatics, Institute of Physics, University of São Paulo, São Carlos, 13560-160, SP, Brazil
[c] Institute of Chemistry, University of Brasilia, P.O. Box 4478, Brasilia, 70904970, DF, Brazil.
[1] These authors contributed equally to this work

Supporting information for this article is given via a link at the end of the document.

Results and Discussion

The new fluorescent imidazole and phenazine derivatives were synthesized as shown in Scheme 2. Quinone-based 1,2,3-triazole (**6**) was prepared by using classical click chemistry methodology and used for the synthesis of the phenazinic compounds.[35] Initially, lapachol (**1**), a natural occurring naphthoquinone was easily extracted from the heartwood of *Tabebuia* sp. (Tecoma),[36] and after recrystallization with appropriate solvent, generally hexane, yellow crystalline solid of **1** was used for converting into nor-lapachol (**2**) via Hooker oxidation reaction.[37] Compound **2** was then treated with bromine affording 3-bromo-nor-β-lapachone, which was followed by nucleophilic substitution with sodium azide in dichloromethane to obtain 3-azido-nor-β-lapachone (**5**) as previously described.[38] Finally, a click reaction with the respective alkyne was used to produce compound **6** in good 70% yield. The structures of **P5** and **6** were solved by using crystallographic methods. Bond lengths and angles are in good agreement with the expected values reported in the literature.[39] Compound **P5** crystallizes with two independent molecules in the asymmetric unit and two water molecules. For clarity, we are showing only one molecule in Scheme 2. The naphthalene and imidazole rings are coplanar and the largest deviation [0.078(2) Å] from the least-square plane is exhibited by atom C1. The dihedral angle between the least-square plane calculated through the atoms of these two rings and [C12-C17] ring is 10.9(3)°. The dihydrofuran ring present a twisted conformation where the puckering parameters calculated for this conformation were: q_2 = 0.287(1) Å, q_3 = 0.581(1) Å, φ_2 = 147.9(2)° , Q = 0.648(3) Å , θ_2 = 26.36°.[40] For compound **6** the atoms of the naphthoquinoidal ring are coplanar and the largest deviation [0.0515(2) Å] from the least-square plane is exhibited by atom C7. Atoms O1 and O2 lie in the mean least-square plane of the quinoidal ring with deviations of 0.0319(1) and 0.0156(1) respectively. Regarding the dihydrofuran ring, the atoms O3, C1 and C12 lie out of the mean least-square plane with deviations of -0.1626(2) Å, -0.1408(1) Å and -0.4833(1) Å respectively and this attribute to furan ring an envelope conformation. The puckering parameters calculated for this conformation were: q_2 = 0.251(1) Å and φ2= 122.5(2)°.[40] The dihedral angle between the least-square plane calculated through the atoms of quinoidal and triazole rings is 86.05(3)°. The least-square plane calculated through the atoms [C16-C29] showing almost planarity and the dihedral angle between this plane and the triazole ring is 135.95(2)°. All H atoms were located by geometric considerations placed (C–H = 0.93-0.97 Å) and refined as riding with U_{iso}(H) = 1.5 U_{eq} (C-methyl) or 1.2 U_{eq} (other). An Ortep-3 diagram of the molecules is shown in Scheme 2 and Table 1 shown the main crystallographic data for **P5** and **6**.

With compound **6** in hands, phenazine **P1** was prepared by the reaction with *ortho*-phenylenediamine. Next, different diamines were prepared by using a reductive sulfur extrusion of substituted 2,1,3-benzothiadiazole (BTD). Initially, π-extended BTDs were prepared following methodology previously described with minor modifications.[41] The substitution pattern of the BTDs was selected aiming electronic conjugation in order to favor the increase of the fluorescence of the subsequent phenazines. The sulfur extrusion from 2,1,3-benzothiadiazole was accomplished by using $NaBH_4$ in the presence of catalytic amounts of $CoCl_2$•$6H_2O$ (1 mol %) as described elsewhere.[42] With the respective substituted diamines in hands, we have synthesized phenazines **P2** and **P3** by the reaction with **6**. Compound **P4** was prepared by cross coupling Sonogashira reaction from dibromide compound **P2**. All attempts for obtaining **P4** from the respective π-extended diamine prepared by Suzuki reaction afforded the product in poor yields.

Naphthoimidazoles derivatives were synthesized by well-know methodology described by Pinto and coworkers.[43] *Ortho*-quinones were used for the synthesis of the fluorescent imidazoles **P5** and **P6**. From lapachol (**1**) and nor-lapachol (**2**), the *ortho*-quinoidal compounds, nor-β-lapachone (**3**) and β-lapachone (**4**) were prepared via acidic cyclization by simple treatment with sulfuric acid. Quinones **3** and **4** were reacted with terephthalaldehyde in acetic acid in the presence of ammonium acetate affording **P5** and **P6**.

Fluorescent phenazine and imidazole derivatives had their photophysical features studied and results are summarized in Table 2 (also see Fig. S37-40 in the ESI file). Phenazines **P1**, **P3** and **P4** showed small Stokes shifts and reasonable molar extinction coefficients with log ε values in the range of 3.79-4.61 mM^{-1} cm^{-1}. Although we have prepared **P2** for preparing **P4**, we have also evaluated their photophysical details, but it was not observed good fluorescence pattern for this nitrogenated heterocycle. In general, probes **P1**, **P3** and **P4** are fluorescent but these data indicate that π-extended phenazinic systems were not as efficient as expected to be.

Imidazole derivatives **P5** and **P6** however displayed large Stokes shifts. In solvents, as for instance, acetonitrile, dichloromethane and dimethyl sulfoxide, we have observed values in the range of 137 to 155 nm. Large molar extinction coefficients (log ε values in the range of 4.11-4.95 mM^{-1} cm^{-1}) were also noted. These data indicates that the **P5** and **P6** have desirable photophysical characteristics to be used as a fluorescent probes for bioimaging. Photophysical details of the compounds in Phosphate-Buffered Saline (PBS, pH = 7.1) was also studied. All the fluorescent probes, with exception of **P1**, have shown similar features as observed for all the aprotic and protic solvents evaluated.

Table 1. Main crystallographic data.

Identification code	Compound **P5**	Compound **6**
Empirical formula	$C_{23}H_{20}N_2O_2$	$C_{29}H_{38}N_3O_3$
Formula weight	744.8	476.6
Temperature	293(2) K	293(2) K
Wavelength	0.71073 Å	0.71073 Å
Crystal system	monoclinic	triclinic
Space group	C2/c	P-1
Unit cell dimensions	a = 32.7465(4) Å α = 90° b = 16.3390(3) Å β = 93.113(4)° c = 14.1742(2) Å γ = 90°	a = 7.4250(4) Å α = 87.198(3)° b = 9.6190(6) Å β = 81.595(4)° c = 21.0910(12) Å γ = 67.245(4)°
Volume	7572.6(3) $Å^3$	1374.2(3) $Å^3$
Z	8	2
Density (calculated)	1.31 Mg/m^3	1.15 Mg/m^3
Absorption coefficient	0.087 mm^{-1}	0.075 mm^{-1}
F(000)	3136	514
Crystal size	0.34 x 0.21 x 0.15 mm^3	0.20 x 0.18 x 0.12 mm^3
Theta range for data collection	2.0 to 26.5°	2.9 to 26.4°
Index ranges	-40≤h≤40, -20≤k≤17, -17≤l≤17	-7≤h1≤7, -9≤k≤10, -22≤l≤22
Reflections collected	28393	7077
Independent reflections	7724 [R(int) = 0.08]	3383 [R(int) = 0.08]
Absorption correction	none	none
Refinement method	Full-matrix least-squares on F^2	Full-matrix least-squares on F^2
Data / restraints / parameters	4792 / 0 / 505	2232 / 0 / 316
Goodness-of-fit on F^2	1.08	1.017
Final R indices [I>2sigma(I)]	R1 = 0.09, wR2 = 0.191	R1 = 0.07, wR2 = 0.181
Largest diff. peak and hole	0.98 and -0.64 e.$Å^{-3}$	0.483 and -0.470 e.$Å^{-3}$

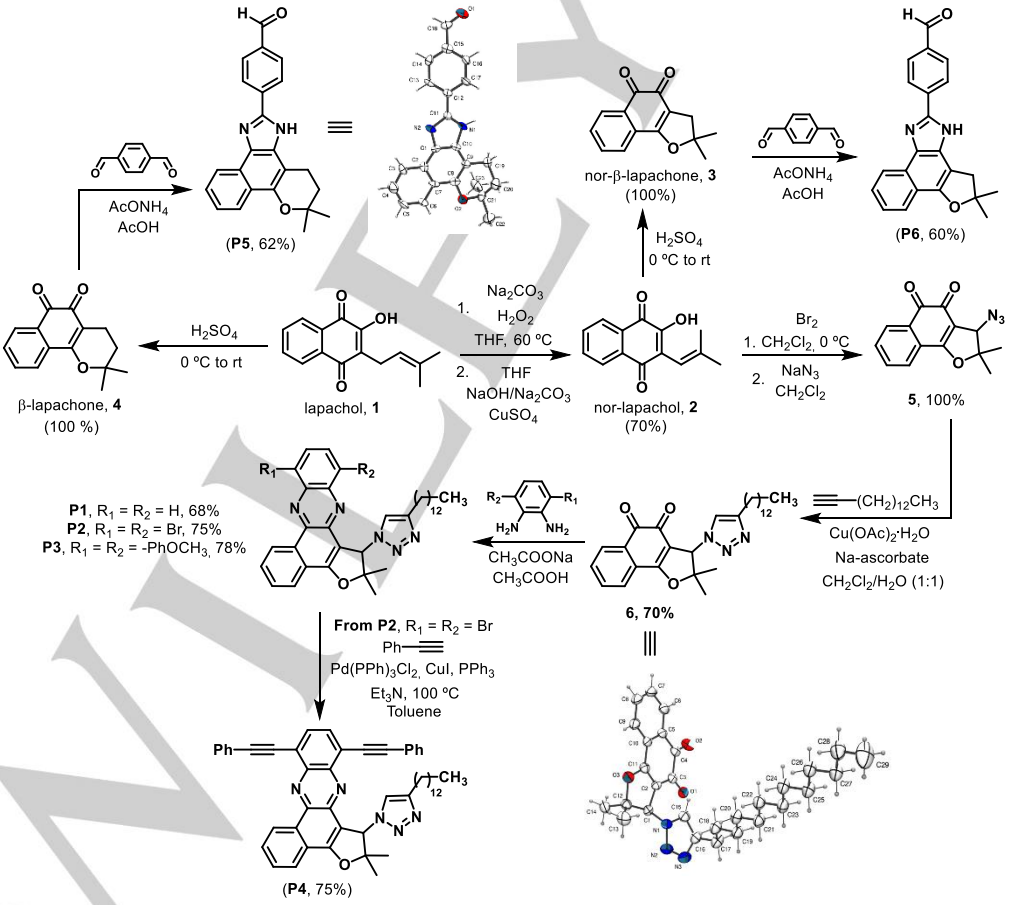

Scheme 2. Synthesis of fluorescent phenazine and oxazole derivatives **P1**-**P6**.

Table 2. Photophysical data (in different solvents) for **P1**, **P3-P6**.

Compounds	Solvent	$\lambda_{max.}$ (abs) (nm)	log ε (ε)	$\lambda_{max.}$ (em) (nm)	Stokes Shift (nm)
	ethyl acetate	425	4.54 (34512)	450	25
	acetonitrile	424	4.51 (32044)	457	33
	dichloromethane	426	4.56 (35923)	448	22
P1	dimethyl sulfoxide	429	4.50 (31762)	469	40
	hexane	424	4.60 (40028)	433	9
	methanol	423	4.55 (35400)	470	47
	toluene	427	4.61 (40720)	443	16
	PBS	nd	nd	nd	nd
	ethyl acetate	411	3.90 (7904)	554	143
	acetonitrile	412	3.79 (6198)	563	151
	dichloromethane	413	3.83 (6738)	555	142
P3	dimethyl sulfoxide	416	3.85 (7132)	572	156
	hexane	411	3.89 (7848)	532	121
	methanol	411	3.82 (6700)	585	174
	toluene	414	3.87 (7366)	547	133
	PBS	434	3.26 (1827)	537	103
	ethyl acetate	421	4.06 (11434)	511	90
	acetonitrile	420	4.03 (10682)	502	82
	dichloromethane	422	4.02 (10554)	514	92
P4	dimethyl sulfoxide	424	4.07 (11864)	511	87
	hexane	421	4.06 (11602)	495	74
	methanol	420	4.03 (2005)	528	108
	toluene	423	4.11 (12846)	507	84
	PBS	425	4.05 (11203)	498	129
	ethyl acetate	401	4.41 (25704)	493	92
	acetonitrile	395	4.50 (31623)	543	148
	dichloromethane	391	4.55 (35481)	523	132
P5	dimethyl sulfoxide	394	4.56 (36308)	545	151
	hexane	390	4.43 (26919)	424	34
	methanol	387	4.39 (24547)	469	82
	toluene	395	4.48 (30200)	487	92
	PBS	389	4.02 (10460)	498	109
	ethyl acetate	392	4.47 (29512)	503	111
	acetonitrile	399	4.51 (32359)	552	153
	dichloromethane	401	4.68 (47863)	538	137
P6	dimethyl sulfoxide	403	4.52 (33113)	558	155
	hexane	395	4.95 (89125)	430	35
	methanol	390	4.60 (39808)	437	47
	toluene	401	4.43 (26915)	488	87
	PBS	395	4.10 (12496)	500	105

Quantum yields (in dichloromethane) for **P1** and **P3**-**P6** of 0.31, 0.62, 0.57, 0.42 and 0.58, respectively. PBS = Phosphate-Buffered Saline (pH = 7.1). nd, Not determined. Photophysical data for **P1** in PBS was not determined due low solubility in all conditions evaluated.

Calculations based on Density Functional Theory (DFT) were carried out at B3LYP[44,45]/TZVP level of theory using the RI approach and the D3 dispersion scheme proposed by Grimme and coworkers.[46] Each structure was fully optimized using a convergence criteria of 10^{-6} Hartree and 10^{-8} Hartree in the SCF calculation. Harmonic frequencies were evaluated for each optimized structure to confirm that it corresponds to a minimum in the potential energy surface. The orbitals were plotted with isovalue of 0.02 e Bohr^{-3}. All calculations were carried out in Orca 3.0.2.[47] DFT calculations were conducted in order to evaluate the frontier orbitals for **P1** and **P3**-**P6**, as shown in Figure 1 and for more details see in the ESI (S41-45). The excited states were evaluated by TD-DFT calculations using the similar theory level described above considering 150 transitions. Our calculations indicate that both HOMO and LUMO orbitals are dispersed in a long extension of the molecules and are basically of π type. The aliphatic side did not show any significant contribution to the frontier orbitals in any molecule, as expected. The HOMO-LUMO band gap was also evaluated for each species. **P5** showed a band gap of 2.7 eV, **P1** was 3.4 eV. **P3**, **P4** and **P6** had band gaps of 3.1 eV. TD-DFT calculations suggest that the first excited state is maily formed by the HOMO - LUMO transition and this transition has a significant contribution to the UV-VIS spectra.

Finally, compounds for **P1** and **P3**-**P6** had their capacity as bioimaging probes evaluated against MCF-7 (human breast adenocarcinoma cells), Caco-2 (human epithelial colorectal adenocarcinoma cells), PANC-1 (human pancreatic carcinoma, epithelial-like cells line) and the T47D (human ductal breast epithelial tumor cells line) and the normal cells HUVEC (human umbilical vein epithelial cells) cells lineage (Figure 2 and Figures S46-S52, in the ESI file). As suggested by the photophysical studies, phenazines **P1**, **P3** and **P4** were not efficient to stain any cellular organelles and could be not visualized inside the cells.

Compounds **P5** and **P6** aldehyde-bearing dyes[48] afforded intense dual fluorescence signals in the ranges of 420-450 nm (blue) and 510-560 nm (green), and it was detected no naked eye photobleaching at the standard operational conditions during the image acquisition process. These compounds were observed distributed near to the nucleus and slightly diffuse through the cells cytoplasm. Both samples conditions (live and fixed cells) showed the same fluorescence pattern. For all Figures the red arrows are indicating the cells regions stained for both compounds and it was also observed difference between fluorescent signal intensities.

Compound **P6** has produced more accentuated fluorescence emission under the same analysis conditions, as can be observed in the confocal microscopy images (Figure 3). However, only the fixed cell samples stained with compound **P6** shows specific marker accumulation near to the nuclei. In the live samples, the staining profile was more diffuse to the cells cytoplasm, Figure 2. No fluorescent signal could be detected in cells nuclei at all experimental conditions, which are noted as black voids inside the cells cytoplasm (Figures 2 and 3). It was also generated phase contrast image for all samples in order to verify the cells morphological aspects. It was observed none morphological alteration for all tested samples related to the short period of cells incubation with these compounds. However, the viability test performed based on 24 hours of cells incubation of these compounds showed different cytotoxic levels depending on the cell type used during the assay. Only when the samples were incubated with 10 µM solution, compound **P5** produced more accentuated cytotoxic effect than those observed in samples treated with **P6**. None cytotoxic effect could be detected in normal cell sample HUVEC treated with the tested compounds at both concentrations. The differences observed between microscopy results and MTT results could be explained by the time of incubation. Results suggest that it is necessary much more than 30 minutes for both compound start to induce cytotoxicity.

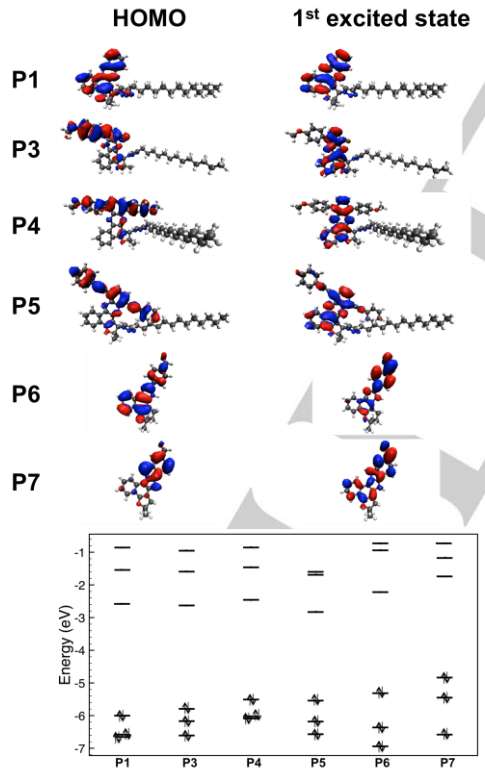

Figure 1. Molecular Orbital Diagram for **P1**, **P3**-**P6** and their respective HOMO orbital and the first excited state calculated at DFT/B3LYP/TZVP and TD-DFT/ B3LYP/TZVP level of theory, respectively, and plotted using an isovalue of 0.02 e Bohr^{-3}.

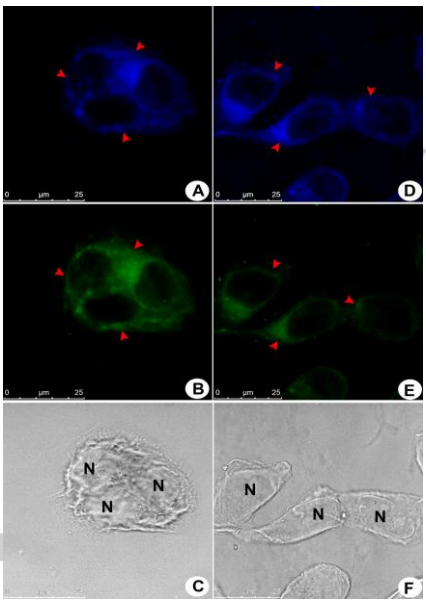

Figure 2. Fluorescent profile of MCF-7 cells, incubated with compound **P5**. Images A, B, D and E show the fluorescent signal distribution to cells cytoplasm in live (A and B) and fixed (D and E) samples. The images C and F show the normal morphological aspects of these samples by phase contrast microscopy. The arrowheads (red) show the distribution of fluorescence in cells cytoplasm. Note the accumulation of fluorescent stain at perinuclear region for both experimental conditions. The "N" letter was used to identify the nuclei. Reference scales bar 25 µm were indicated.

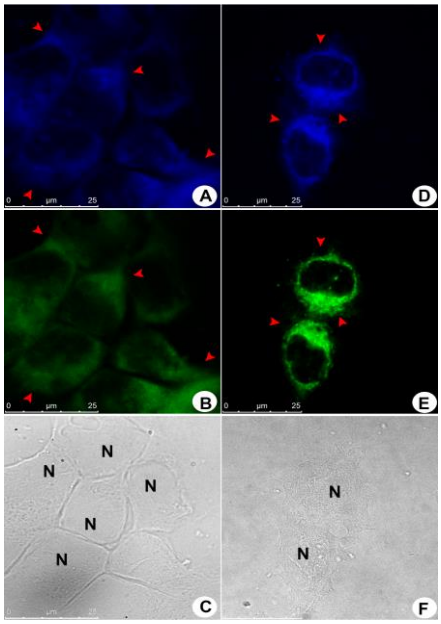

Figure 3. Fluorescent profile of MCF-7 cells, incubated with compound **P6**. Images A, B, D and E show the fluorescent signal distribution to cells cytoplasm in live (A and B) and fixed (D and E) samples. The images C and F show the normal morphological aspects of these samples by phase contrast microscopy. The arrowheads (red) show the distribution of fluorescence in cells cytoplasm. Note a more intense fluorescence emission and specific staining accumulation in perinuclear region in fixed cells sample. The "N" letter was used to identify the nuclei. Reference scales bar 25 µm were indicated.

In order to confirm that the observed fluorescent patterns are correlated with the mitochondria staining it was performed a cells staining by using MitotrackerTM, which is a widely used commercial marker of mitochondria. The fluorescent signal pattern observed in mammal cells using **P5** and **P6** were identical to the fluorescent pattern obtained from MitotrackerTM staining assay. Both compounds and the MitotrackerTM were observed accumulated near to the cells nuclei and slight distributed in cells cytoplasm, which is the typical mitochondria distribution in this line cell model. The results obtained by MitotrackerTM cells staining confirmed our preview finds that **P5** and **P6** could stain mitochondria selectively. Figure 4 shows the cell cytoplasm fluorescence distribution in samples stained with **P5** and **P6** (green) and with MitotrackerTM (red). It was also produced an image from the fluorescence channel overlay from each tested compound and MitotrackerTM (images B). The white arrows are indicating the region of staining accumulation in the cells cytoplasm for both compounds, which is the same observed by the MitotrackerTM staining. The images created through the overlay fluorescence channels (Figure 4, images B), which combined the green emission from compounds **P5** or **P6** (green) and red emission from (Mitotracker), produced a yellow color. The yellow color demonstrated that the both signal are emitted from the same cell region, which means from the mitochondria. These results demonstrated that the compound **P5** and **P6** could be applied as new mitochondria marker, permeable to the cell membrane. It was also generated phase contrast image for all samples (images D) in order to verify the cells morphological aspects and it was observed no morphological alteration in MCF-7 cells submitted to dual staining procedures. Finally, we have also accomplished colocalization analysis (Pearson's correlation coefficient) with **P5** or **P6** and MitotrackerTM. Data were inserted in the Supplementary Information (Figure S54).

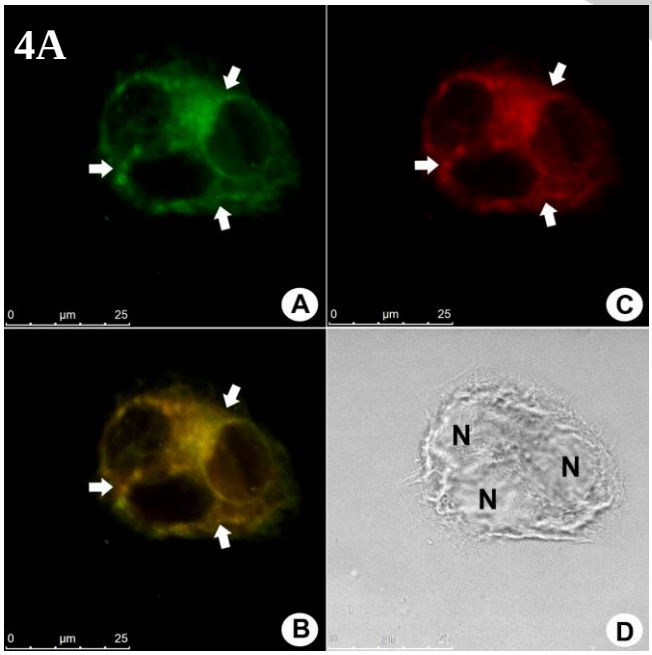

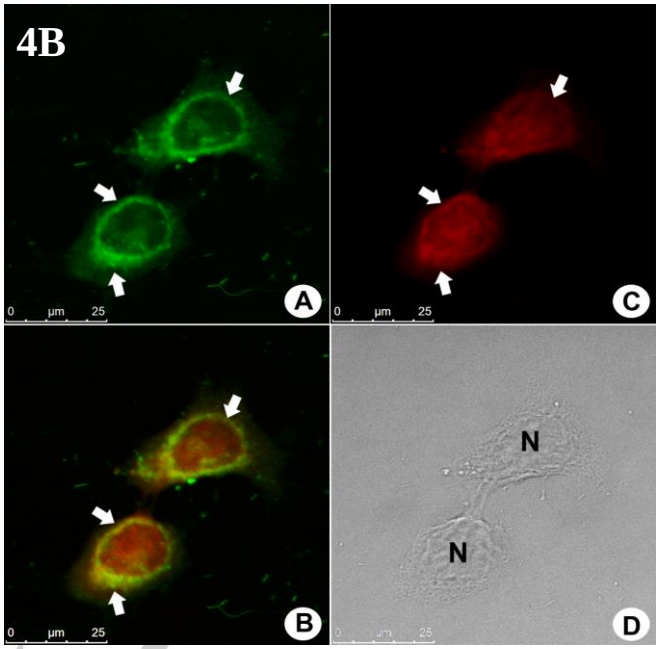

Figure 4. Fluorescent profile of MCF-7 cells incubated with compound **P5** (**4A**) and **P6** (**4B**) plus MitotrackerTM. The images A show the staining profile obtained from **P5** (**4A**) and **P6** (**4B**) and the images C shows the staining profile from MitotrackerTM. The white arrows are indicating the perinuclear staining accumulation for all markers used. Images B were produced by the overlay of the green and red fluorescence images, the yellow color produced demonstrate that there is an overlap between the fluorescence emission from the tested compounds and the MitotrackerTM. The images D shows the normal morphological aspects of the samples by phase contrast microscopy. The cells nuclei were identified by "N" letter in images D. Reference scale bar 25 µm.

Conclusions

Five new fluorescent compounds were prepared from lapachol, a naturally occurring naphthoquinone, easily extracted from ipe tree. Two of these compounds, imidazole derivatives, were very efficient to selectively stain mitochondria. To the best of our knowledge, this is the first report with azoles prepared from a natural product with highlighted luminescence prepared in only three or four steps that are able to use as selective mitochondrial imaging probes. This manuscript opens a new avenue for the synthesis and application of fluorescent compounds prepared from natural compounds, as for instance, lapachones.

Experimental Section

Chemistry. Melting points were obtained on Thomas Hoover and are uncorrected. Analytical grade solvents were used. Column chromatography was performed on silica gel (SiliaFlash G60 UltraPure 60–200 mm, 60 Å). Infrared spectra were recorded on an FTIR Spectrometer IR Prestige-21 Shimadzu. ^{1}H and ^{13}C NMR spectra were recorded at 303 K using a Bruker AVANCE DRX400 spectrometer. All samples for NMR were prepared in $CDCl_3$ containing TMS as internal reference. Chemical shifts (δ) are given in ppm and coupling constants

(*J*) in hertz. High resolution mass spectra (electrospray ionization) were obtained using a MicroTOF Ic – Bruker Daltonics instrument.

General procedure for the extraction of lapachol (**1**) from the heartwood of *Tabebuia* sp. (Tecoma): A saturated aqueous sodium carbonate solution was added to the sawdust of *ipê* tree. Upon observing rapid formation of lapachol sodium salt, hydrochloric acid was added, allowing the precipitation of lapachol. Then, the solution was filtered and a yellow solid was obtained. This solid was purified by recrystallizations with hexane.

Nor-lapachol (2) was synthesized by Hooker oxidation methodology and data are consistent with those reported in the literature.[11,49] Compound **2** was obtained as an orange solid (160 mg, 0.7 mmol, 70% yield); mp 121-122 ºC. ^{1}H NMR (400 MHz, $CDCl_3$, 303 K) *δ*: 8.13 (ddd, *J* = 7.5, 1.5 and 0.5 Hz, 1H), 8.10 (ddd, *J* = 7.5, 1.5 and 0.5 Hz, 1H), 7.76 (td, *J* = 7.5, 7.5 and 1.5 Hz, 1H), 7.69 (td, *J* = 7.5, 7.5 and 1.5 Hz, 1H), 6.03-5.99 (m, 1H), 2.0 (d, *J* = 1.5 Hz, 3H), 1.68 (d, *J* = 1.2 Hz, 3H). ^{13}C NMR (100 MHz, $CDCl_3$, 303 K) d: 184.7, 181.5, 151.1, 143.6, 134.9, 133.0, 132.9, 129.5, 126.9, 126.0, 120.9, 113.6, 26.5, 21.7.

General procedure for the synthesis of nor-β-lapachone (3) and β-lapachone (4). Sulfuric acid was slowly added to lapachol (**1**) or nor-lapachol (**2**) (1 mmol) until complete dissolution of the quinone. Then, the solution was poured into ice and the precipitate formed was filtered and washed with water. Lapachones (**3**) and (**4**) were recrystallized in an appropriate solvent, as for instance, ethanol. Compound **3** and **4** were obtained as an orange solids. Nor-β-lapachone (**3**): Nor-β-lapachone was obtained as an orange solid (216 mg, 95% yield); m.p. 169-171 ºC. ^{1}H NMR (400 MHz, $CDCl_3$, 303 K) *δ*: 8.05-803 (m, 1H), 7.66-7.52 (m, 3H), 2.93 (s, 2H), 1.60 (s, 6H). ^{13}C NMR (100 MHz, $CDCl_3$, 303 K) *δ*: 181.3, 175.6, 168.7, 134.4, 131.8, 130.9, 129.2, 127.9, 124.5, 115.0, 93.7, 39,3, 28.4. Data are consistent with those reported in the literature.[50] β-lapachone (**4**): (240 mg, 99% yield); mp 153-155 ºC. ^{1}H NMR (400 MHz, $CDCl_3$, 303 K) *δ*: 8.06 (dd, *J* = 7.6 and 1.4 Hz, 1H), 7.81 (dd, *J* = 7.8 and 1.1 Hz, 1H), 7.65 (ddd, *J* = 7.8, 7.6 and 1.4 Hz, 1H), 7.51 (td, *J* = 7.6, 7.6 and 1.1 Hz, 1H), 2.57 (t, *J* = 6.7 Hz, 2H), 1.86 (t, *J* = 6.7 Hz, 2H), 1.47 (s, 6H). ^{13}C NMR (100 MHz, $CDCl_3$, 303 K) *δ*: 179.8, 178.5, 162.0, 134.7, 132.6, 130.6, 130.1, 128.5, 124.0, 112.7, 79.3, 31.6, 26.8, 16.2. Data are consistent with those reported in the literature.[51]

Synthesis of 3-azido-2,2-dimethyl-2,3-dihydronaphtho[1,2-b]furan-4,5-dione (5). To a solution of nor-lapachol (**2**) (228 mg, 1.0 mmol) in 25 mL of dichloromethane, 2 mL of bromine was added. The bromo intermediate precipitated immediately as an orange solid. After removal of bromine, an excess of sodium azide (2 mmol) was added in CH_2Cl_2 and the mixture was stirred overnight. The crude reaction mixture was poured into 50 mL of water. The organic phase was extracted with organic solvent, dried over sodium sulfate, filtered, and evaporated under reduced pressure. Compound **5** was obtained as an orange solid (263 mg, 0.98 mmol, 98% yield); mp 200-202 ºC. ^{1}H NMR (400 MHz, $CDCl_3$, 303 K) *δ*: 8.14 (ddd, *J* = 6.9, 2.1 and 0.9 Hz, 1H), 7.72-7.65 (m, 3H), 4.77 (s, 1H), 1.67 (s, 3H), 1.55 (s, 3H). ^{13}C NMR (100 MHz, $CDCl_3$, 303 K) *δ*: 180.3, 175.2, 170.2, 134.5, 132.7, 131.1, 113.5, 129.5, 125.1, 126.7, 95.5, 67.3, 27.1, 21.9. Data are consistent with those reported in the literature.[52]

2,2-dimethyl-3-(4-tridecyl-1*H*-1,2,3-triazol-1-yl)-2,3-dihydronaphtho[1,2-*b*]furan-4,5-dione (6). Click chemistry procedure was used for preparing compound **6** as previously classical methodology described by Sharpless and Fokin with minor modifications.[35] In a 25 mL flask containing 15 mL of CH_2Cl_2/H_2O (1:1), $Cu(OAc)_2{\cdot}H_2O$ (10 mg, 0.08 mmol) and sodium ascorbate (30 mg, 0.15 mmol), was added 3-azido-nor-β-lapachone (135 mg, 0.5 mmol) and 1-pentadecyne (217 mg, 0.28 mL, 1.0 mmol). The mixture was stirred at room temperature, and, the reaction was monitored by thin layer chromatography. The aqueous phase was extracted with CH_2Cl_2, dried over anhydrous Na_2SO_4 and concentrated under reduced pressure. The residue was purified by column chromatography using as eluent a mixture of hexane/ethyl acetate, with a gradient of increasing polarity. The product was obtained as an orange solid (166 mg, 0.7 mmol, 70% yield); mp 111-112 ºC. ^{1}H NMR (400 MHz, $CDCl_3$, 303 K) *δ*: 8.16 (dd, *J* = 7.4 and 1.2 Hz, 1H), 7.81-7.66 (m, 3H), 7.21 (s, 1H), 5.92 (s, 1H), 2.69-2.60 (t, *J* = 8.0 Hz, 2H), 1.73 (s, 3H), 1.68-1.53 (m, 2H), 1.34-1.18 (m, 20H), 1.16 (s, 3H), 0.86 (t, 3H, *J* = 6.9 Hz). ^{13}C NMR (100 MHz; $CDCl_3$, 303 K) *δ*: 180.1, 174.4, 171.1, 148.3, 134.8, 133.2, 131.5, 129.9, 126.7, 125.5, 120.1, 111.4, 96.0, 66.6, 44.3, 31.9, 29.6, 29.6, 29.6, 29.5, 29.3, 29.3, 29.2, 27.6, 25.6, 22.6, 21.0, 14.0. EI/HRMS (m/z) $[M+H]^+$: 478.3065. Cald for $[C_{29}H_{40}N_3O_3]^+$: 478.3069.

General Procedure for the synthesis of the phenazines. In a 25 mL flask, quinone **6** (0.5 mmol), sodium acetate (0.95 mmol), the respective diamine (0.55 mmol) in 3 mL of glacial acetic acid were added. The reaction medium was agitated at room temperature and monitored by thin layer chromatography. After, the crude reaction was poured into water and the precipitate formed was filtrate and then purified by column chromatography on silica gel eluted with an increasing polarity gradient mixture of hexane and ethyl acetate.

2,2-dimethyl-1-(4-tridecyl-1*H*-1,2,3-triazol-1-yl)-1,2-dihydrobenzo[*a*]furo[2,3-*c*]phenazine (P1). Compound **P1** was obtained as yellow solid (186 mg, 0.34 mmol, 68% yield); mp 151-153 ºC. ^{1}H NMR (400 MHz, $CDCl_3$, 303 K) *δ*: 9.46 (dd, *J* = 8.0 and 0.7 Hz, 1H), 8.32-8.27 (m, 1H), 8.21 (dd, *J* = 7.8 and 0.9 Hz, 1H), 8.09-8.03 (m, 1H), 7.91 (dtd, *J* = 24.7, 7.3 and 1.3 Hz, 2H), 7.80-7.73 (m, 2H), 6.87 (s, 1H), 6.66 (s, 1H), 2.64-2.48 (m, 2H), 1.80 (s, 3H), 1.56-1.43 (m, 2H), 1.29 (s, 3H), 1.26-1.05 (m, 20H), 0.87 (t, *J* = 6.9 Hz, 3H). ^{13}C NMR (100 MHz, $CDCl_3$, 303 K) *δ*: 148.0, 140.9, 140.4, 133.2, 130.3, 130.0, 129.8, 129.6, 128.7, 126.1, 124.1, 123.2, 120.1, 108.9, 92.9, 68.4, 31.9, 29.6, 29.6, 29.5, 29.5, 29.4, 29.3, 29.2, 29.0, 27.5, 25.6, 22.6, 21.3, 14.1. EI/HRMS (m/z) $[M+H]^+$: 550.3518. Cald for $[C_{35}H_{44}N_5O]^+$: 550.3545.

9,12-dibromo-2,2-dimethyl-1-(4-tridecyl-1*H*-1,2,3-triazol-1-yl)-1,2-dihydrobenzo[*a*]furo[2,3-*c*]phenazine (P2). Compound **P2** was obtained as yellow solid (264 mg, 0.37 mmol, 75% yield); mp 142-143 ºC. ^{1}H NMR (400 MHz, $CDCl_3$, 303 K) *δ*: 9.52 (d, *J* = 7.7 Hz, 1H), 8.25 (d, *J* = 7.3 Hz, 1H), 7.99-7.88 (m, 4H), 6.99 (s, 1H), 6.68 (s, 1H), 2.61 (t, *J* = 7.3 Hz, 2H), 1.87 (s, 3H), 1.60-1.46 (m, 2H), 1.37 (s, 3H), 1.28-1.07 (m, 20H), 0.89 (t, *J* = 6.9 Hz, 3H). ^{13}C NMR (100 MHz, $CDCl_3$, 303 K) *δ*: 161.3, 147.8, 142.4, 141.6, 140.6, 138.0, 133.1, 132.5, 131.6, 130.7, 130.2, 127.0, 124.5, 124.2, 123.4, 123.4, 120.3, 108.8, 93.3, 68.5, 31.9, 29.6, 29.6, 29.6, 29.5, 29.4, 29.3, 29.2, 29.0, 28.0, 25.6, 22.6, 21.6, 14.0. EI/MS (m/z) $[M+H]^+$: 706. Cald for $[C_{35}H_{42}Br_2N_5O]^+$: 706.

9,12-bis(4-methoxyphenyl)-2,2-dimethyl-1-(4-tridecyl-1*H*-1,2,3-triazol-1-yl)-1,2-dihydrobenzo[*a*]furo[2,3-*c*]phenazine (P3). Compound **P3** was obtained as yellow solid (296 mg, 0.39 mmol, 78% yield); mp 163-165 ºC. ^{1}H NMR (400 MHz, $CDCl_3$, 303 K) *δ*: 9.21-9.15 (m, 1H), 8.20-8.14 (m, 1H), 7.92-7.79 (m, 6H), 7.30 (d, *J* = 8.7 Hz, 2H), 7.15 (d, *J* = 8.7 Hz, 2H), 6.97 (d, *J* = 8.7 Hz, 2H), 6.87 (s, 1H), 6.53 (s, 1H), 3.97 (s, 3H), 3.94 (s, 3H), 2.61 (t, *J* = 7.7 Hz, 2H), 1.75 (s, 3H), 1.59-1.45 (m, 2H), 1.28 (s, 3H), 1.23-1.02 (m, 20H), 0.86 (t, *J* = 6.9 Hz, 3H). ^{13}C NMR (100 MHz, $CDCl_3$, 303 K) δ: 160.0, 159.2, 148.0, 140.5, 140.2, 139.6, 139.1, 138.4, 138.0, 133.5, 132.2, 131.7, 131.3, 130.1, 129.7, 129.5, 128.5, 126.4, 124.2, 123.0, 119.8, 113.7, 113.4, 108.9, 92.7, 68.6, 55.4, 55.4, 31.9, 29.6, 29.6, 29.5, 29.5, 29.4, 29.4, 29.3, 29.2, 29.1, 27.7, 25.6, 22.6, 21.5, 14.0. EI/HRMS (m/z) $[M+H]^+$: 762.4344. Cald for $[C_{49}H_{56}N_5O_3]^+$: 762.4383.

2,2-dimethyl-9,12-bis(phenylethynyl)-1-(4-tridecyl-1*H*-1,2,3-triazol-1-yl)-1,2-dihydrobenzo[*a*]furo[2,3-*c*]phenazine (P4). In a 25 mL schlenk tube were added **P2** (0.07 mmol), phenylacetylene (0.28 mmol), $Pd(Ph_3)_2Cl_2$ (0.05 mmol), triphenylphosphine (0.1 mmol) and copper(I) iodide (0.05 mmol). The tube was evacuated and backfilled with nitrogen. Triethylamine (5.0 mL) was added under nitrogen, and the tube was locked. The tube was immersed in an oil bath (90 °C) and stirred for 12 h. After, the solvent was evaporated and the product purified by column chromatography on silica gel using a mixture of hexane/ethyl acetate. **P4** was obtained as a orange solid (280 mg, 0.37 mmol, 75% yield); mp 132-134 ºC; ^{1}H NMR (400 MHz, $CDCl_3$, 303 K) *δ*: 9.58 (d, *J* = 7.9 Hz, 1H),

8.23 (d, *J* = 7.5 Hz, 1H), 8.01-7.94 (m, 3H), 7.90 (t, *J* = 7.1 Hz, 1H), 7.79 (d, *J* = 6.5 Hz, 2H), 7.61 (d, *J* = 7.2 Hz, 2H), 7.52-7.43 (m, 5H), 7.42-7.36 (m, 1H), 6.90 (s, 1H), 6.73 (s, 1H), 2.58-2.47 (m, 2H), 1.82 (s, 3H), 1.48-1.37 (m, 2H), 1.32 (s, 3H), 1.29-1.00 (m, 20H), 0.86 (t, *J* = 6.8 Hz, 3H). ^{13}C NMR (100 MHz, $CDCl_3$, 303 K) *δ*: 160.9, 147.7, 142.5, 142.0, 141.0, 140.1, 133.1, 133.1, 132.2, 131.9, 130.3, 130.0, 128.7, 128.7, 128.5, 128.4, 126.5, 124.4, 123.8, 123.5, 123.3, 123.3, 123.0, 120.3, 108.9, 98.0, 97.5, 93.4, 87.0, 86.2, 68.4, 31.9, 29.6, 29.6, 29.6, 29.5, 29.4, 29.3, 29.2, 28.8, 27.8, 25.5, 22.6, 21.4, 14.0. EI/HRMS (m/z) $[M+H]^+$: 750.4146. Cald for $[C_{51}H_{52}N_5O]^+$: 750.4171.

4-(6,6-dimethyl-3,4,5,6-tetrahydrobenzo[7,8]chromeno[5,6-d]imidazol-2-yl)benzaldehyde (P5). To a solution of β-lapachone (1.0 mmol, 242 mg) in acetic acid (10 mL), terephthalaldehyde (3.0 mmol, 402 mg) was added, and the mixture was heated to 70 ºC; at this point, ammonium acetate (20.0 mmol, 1.54 g) was slowly added, and reflux was maintained for 2h. At the end of the reaction, after addition into cold water, a yellow precipitate was formed and filtered under reduced pressure. The precipitate was also washed with distilled water and a solution of sodium bicarbonate. Finally, it was purified by column chromatography using as eluent a mixture of hexane/ethyl acetate, with a gradient of increasing polarity, as previously described. Compound **P5** was obtained as a yellow solid (220 mg, 0.6 mmol, 62% yield); mp 271-272 ºC. ^{1}H NMR (400 MHz, $CDCl_3$/DMSO-d_6, 303 K) *δ*: 10.00 (s, 1H), 8.49 (d, *J* = 7.7 Hz, 1H), 8.42 (d, *J* = 7.9 Hz, 2H), 8.26 (d, *J* = 7.8 Hz, 1H), 7.92 (d, *J* = 7.9 Hz, 2H), 7.54 (t, *J* = 7.7 Hz, 1H), 7.44 (t, *J* = 7.8 Hz, 1H), 3.11 (t, *J* = 5.9 Hz, 2H), 1.99 (t, *J* = 5.9 Hz, 2H), 1.46 (s, 6H). ^{13}C NMR (100 MHz, $CDCl_3$/DMSO-d_6, 303 K) *δ*: 191.2, 146.9, 145.2, 136.1, 135.3, 129.6, 126.2, 125.5, 123.5, 122.3, 121.1, 103.7, 74.0, 31.7, 26.3, 18.4. EI/HRMS (m/z) $[M+H]^+$: 357.1584. Cald for $[C_{23}H_{20}N_2O_2]^+$: 357.1558.

4-(5,5-dimethyl-4,5-dihydro-3H-furo[3',2':3,4]naphtho[1,2-d]imidazol-2-yl)benzaldehyde (P6). To a solution of nor-β-lapachone (1.0 mmol, 228 mg) in acetic acid (10 mL), terephthalaldehyde (3.0 mmol, 402 mg) was added, and the mixture was heated to 70 ºC; at this point, ammonium acetate (20.0 mmol, 1.54 g) was slowly added, and reflux was maintained for 3h. At the end of the reaction, after addition into cold water, a yellow precipitate was formed and filtered under reduced pressure. The precipitate was also washed with distilled water and a solution of sodium bicarbonate.[43,53] Finally, it was purified by column chromatography using as eluent a mixture of hexane/ethyl acetate, with a gradient of increasing polarity. Compound **P6** was obtained as a yellow solid (205 mg, 0.6 mmol, 60% yield); mp 268-269 ºC. ^{1}H NMR (400 MHz, $CDCl_3$/DMSO-d_6, 303 K) *δ*: 10.00 (s, 1H), 8.55 (d, *J* = 7.4 Hz, 1H), 8.40 (d, *J* = 7.8 Hz, 2H), 8.03 (d, *J* = 7.7 Hz, 1H), 7.92 (d, *J* = 7.8 Hz, 2H), 7.54 (t, *J* = 7.4 Hz, 1H), 7.44 (t, *J* = 7.7 Hz, 1H), 3.38 (s, 2H), 1.61 (s, 6H). ^{13}C NMR (100 MHz, $CDCl_3$/DMSO-d_6, 303 K) *δ*: 191.5, 151.8, 147.3, 136.2, 135.7, 129.9, 126.4, 125.7, 123.9, 122.5, 121.9, 118.9, 106.6, 87.5, 42.0, 28.4. EI/HRMS: (m/z) $[M+H]^+$: 343.1448. Cald for $[C_{22}H_{18}N_2O_2]^+$: 343.1339.

Biology. Cell culture. MCF-7 (human breast adenocarcinoma cell), Caco2 (human epithelial colorectal adenocarcinoma cells), PANC-1 (human pancreatic carcinoma, epithelial-like cell line) and the T47D (human ductal breast epithelial tumor cell line) and the normal cell HUVEC (human umbilical vein epithelial cell) were used in this work. The cells were maintained in appropriated culture medium as recommended by ATCC (American Type Culture Collection), supplemented with 10% of fetal bovine serum plus 100 IU/mL penicillin and 100 µg/mL streptomycin at 37 °C in 5% CO_2 atmosphere.

Fluorescence detection assay. Cells were seeded on 13mm round glass coverslips on the bottom of a 24-well plate, allowed to adhere overnight and washed three times with serum-free medium for removal of non-adherent cells. After reaching confluence, the cells were separated in two samples (live samples and fixed samples). The live samples were incubated for 30 minutes in 1 µM of **P5** or **P6** solution at 37 °C. These samples were washed three times with PBS 1X (pH 7.4) at room temperature and fixed in formaldehyde 3.7% for 30 minutes. The samples were washed again three times in PBS 1X (pH 7.4) at room temperature and the coverslips were mounted over glass slides using ProLong Gold Antifade (Invitrogen, OR, USA) according to the manufacturer's recommendations. The fixed samples were first washed three times in PBS 1X (pH 7.4) and then fixed with formaldehyde 3.7% for 30 minutes. After fixative procedure the samples were washed three times in PBS 1X (pH 7.4) at room temperature and incubated for 30 minutes in 1 µM of **P5** or **P6** solution at room temperature. The samples were washed three times in PBS 1X (pH 7.4) at room temperature and the coverslips were mounted over glass slides using ProLong Gold Antifade (Invitrogen, OR, USA) according to the manufacturer's recommendations. The negative control was performed by incubation of the samples in 0.02% of DMSO, which was the diluent used. The samples were analyzed using a Leica Confocal Microscopy TCS SP5 and excited using 488 nm wavelength laser emission. All assays were performed in triplicate and it was done three repetitions for each cell sample and experimental condition.

Cell viability assay. The same cell lineages used in fluorescence detection assay were incubated with **P5** or **P6** solutions at 1 or 10 µM for 24 hours and analyzed by standard MTT (3-[4, 5-dimethylthiazol-2-yl]-2, 5-diphenyltetrazolium bromide) assay, following the manufacture recommendations (R&D System Inc, MN, USA). Briefly, 3 x 10^3 of each cell line were seeded in 96 well plate and maintained overnight a 37 °C. These samples were incubated in 1 or 10 µM of **P5** or **P6** solutions for 24 hours. Cells incubated with 0.02% of DMSO solution (compound solvent) at the same conditions and cells maintained only in culture medium were used as diluent control and negative control respectively. The samples were incubated with 150 µL of MTT solution (0.5 mg/mL) in cell culture medium for 4h, in the dark at 37 °C. MTT is reduced by metabolically active cells to insoluble purple formazan dye crystals which were accumulated inside the cells cytoplasm. The MTT solution was removed and was add 200 µL of DMSO in all samples in order to solubilize the formazan dye crystals. The plate was read in spectrophotometer Spectramax M5 (Molecular Devices, CA, USA) and the optimal wavelength for absorbance was 570 nm. The MTT assay was performed in triplicate and also was made three independent assays. The cell viability inhibition was determined by evaluation of MTT result obtained for test samples compared with the control samples in the same conditions, following the expression [Survival % = [(Tested Sample – Blanc)/(Control Sample – Blanc)] x 100. The data was statically analyzed by ANOVA one way test followed to Dunnett's post test.

Co-staining P5, P6 and Mitotracker. In order to confirm the morphological evidence that the compounds **P5** or **P6** was accumulated in mitochondria, it was performed a co-staining assay with each compound and the commercial mitochondria marker MitotrackerTM (ThermoFisher Scientific, NY, USA). Briefly, 3 x 10^5 MCF-7 cells (human breast adenocarcinoma cell), were seeded on 13 mm round glass coverslips on the bottom of a 24-well plate, allowed to adhere overnight and washed three times with serum-free medium for removal of non-adherent cells. After reaching confluence, the samples were incubated for 30 minutes at 37 °C with 1 µM of **P5** or **P6** plus 100 nM of MitotrackerTM. The samples were washed three times in PBS (Phosphate Buffer Saline), pH 7.4 at 37 °C and the cells were fixed in 3.7% formaldehyde solution for 30 minutes at room temperature. The samples were washed three times in PBS and the coverslips were mounted over glass slides using ProLong Gold Antifade (Invitrogen, OR, USA) according to the manufacturer's recommendations. The samples were analyzed using a Leica Confocal Microscopy TCS SP5. All assays were performed in triplicate and it was done in three independent repetitions

X-ray. The structures of the title compounds has been determined from X- ray diffraction on an Enraf-Nonius Kappa-CCD diffractometer (95 mm CCD camera on κ-goniostat) using graphite monochromated MoKα

radiation (0.71073 Å), at room temperature. Data collections were carried out using the COLLECT software[54] up to 50° in 2θ. Final unit cell parameters were based on 12320 reflections for **P5** and 3373 reflections for **6**. Integration and scaling of the reflections, correction for Lorentz and polarization effects were performed with the HKL DENZO-SCALEPACK system of programs.[55] The structures of compounds were solved by direct methods with SHELXS-97.[56] The models were refined by full-matrix least squares on F2 using SHELXL-97.[57] The program ORTEP-3[58] was used for graphic representation and the program WINGX[59] to prepare materials for publication. The reference number is CCDC 1529639 and 1530427. Copies of the available material can be obtained, free of charge on application to the Director, CCDC, 12 Union Road, Cambridge CH21EZ, UK (fax: +44-1223-336-033 or e-mail: deposit@ccdc.cam.ac.uk or http://www.ccdc.cam.ac.uk).

Acknowledgements

This research was funded by grants from CNPq (PVE 401193/2014-4), FAPEMIG (Edital 01/2014), Chamada universal MCTI/CNPq Nº 01/2016 and 474797/2013-9, Programa Pesquisador Mineiro PPM-X FAPEMIG, CAPES, FAPDF, FINATEC, DPP-UnB, INCT-Transcend group. Prof. C.A.S. would like to thank the Institute of Physics of University of São Paulo (São Carlos), for kindly allowing the use of the KappaCCD diffractometer.

Keywords: Quinones 1 • Heterocycles 2 • Probes 3 • Fluorescence 4 • Redox Modification 5

[1] F. E. Koehn, G. T.Carter, *Nat. Rev. Drug Discov.* **2005**, *4*, 206-220.

[2] (a) E. N. da Silva Júnior, G. A. M. Jardim, R. F. S. Menna-Barreto, S. L. de Castro, *J. Braz. Chem. Soc.* **2014**, *25*, 1780-1798; (b) A. A. Vieira, J. B. Azeredo, M. Godoi, C. Santi, E. N. da Silva Júnior, A. L. Braga, *J. Org. Chem.* **2015**, *80*, 2120-2127.

[3] K. W. Wellington, *RSC Adv.* **2015**, *5*, 20309-20338.

[4] (a) K. C. G. De Moura, F. S. Emery, C. N. Pinto, M. C. F. R. Pinto, A. P. Dantas, K. Salomão, S. L. de Castro, A. V. Pinto, *J. Braz. Chem. Soc.* **2001**, *12*, 325-338; (b) C. Salas, R. A. Tapia, K. Ciudad, V. Armstrong, M. Orellana, U. Kemmerling, J. Ferreira, J. D. Maya, A. Morello, *Bioorg. Med. Chem.* **2008**, *16*, 668-674.

[5] (a) S. Bannwitz, D. Krane, S. Vortherms, T. Kalin, C. Lindenschmidt, N. Z. Golpayegani, J. Tentrop, H. Prinz, K. Müller, J. Med. Chem. **2014**, *57*, 6226-6239; (b) C. P. V. Freire, S. B. Ferreira, N. S. M. de Oliveira, A. B. J. Matsuura, I. L. Gama, F. C. da Silva, M. C. B. V. de Souza, E. Silva Lima, V. F. Ferreira, *Med. Chem. Commun.* **2010**, *1*, 229-232; (c) N. B. de Souza, I. M. de Andrade, P. F. Carneiro, G. A. M. Jardim, I. M. M. de Melo, E. N. da Silva Júnior, A. U. Krettli, *Mem. Inst. Oswaldo Cruz* **2014**, *109*, 546-552.

[6] S. G. C. Fonseca, R. M. C. Braga, D. P. Santana, *Rev. Bras. Farm.* **2003**, *84*, 9-16.

[7] S. L. de Castro, F. S. Emery, E. N. da Silva Júnior, Eur. *J. Med. Chem*. **2013**, *69*, 678-700.

[8] C. E. M. Carvalho, N. C. de Lucas, J. O. M. Herrera, A. V. Pinto, M. C. F. R. Pinto, I. M. Brinn, *J. Photochem. Photobiol. A: Chem.* **2004**, *167*, 1-9.

[9] F. S. Emery, M. C. F. R. Pinto, C. A. de Simone, V. R. S. Malta, E. N. da Silva Júnior, A. V. Pinto, *Synlett*, **2010**, *13*, 1931-1934.

[10] G. G. Dias, P. V. B. Pinho, H. A. Duarte, J. M. Resende, A. B. B. Rosa, J. R. Correa, B. A. D. Neto, E. N. da Silva Júnior, *RSC Adv*. **2016**, *6*, 76056-76063.

[11] G. G. Dias, B. L. Rodrigues, J. M. Resende, H. D. R. Calado, C. A. de Simone, V. H. C. Silva, B. A. D. Neto, M. O. F. Goulart, F. R. Ferreira, A. S. Meira, C. Pessoa, J. R. Correa, E. N. da Silva Júnior, *Chem. Commun*. **2015**, *51*, 9141-9144.

[12] G. A. M. Jardim, H. D. R. Calado, L. A. Cury, E. N. da Silva Júnior, *Eur. J. Org. Chem.* **2015**, *4*, 703-709.

[13] B. B. Costa, G. A. M. Jardim, P. L. Santos, H. D. R. Calado, A. P. Monkman, F. B. Dias, E. N. da Silva Júnior, L. A. Cury, *Phys. Chem. Chem. Phys.* **2017**, *19*, 3473-3479.

[14] P. Prasad, I. Khan, P. Kondaiah, A. R. Chakravarty, *Chem. Eur. J.* **2013**, *19*, 17445-17455.

[15] Y. Ding, Q. Wu, K. Zheng, L. An, X. Hu, W. Mei, *RSC Adv.* **2015**, *5*, 63330-63337.

[16] T. Sarkar, S. Banerjee, A. Hussain, *RSC Adv.* **2015**, *5*, 16641-16653.

[17] S. Saha, A. Ghosh, P. Mahato, S. Mishra, S. K. Mishra, E. Suresh, S. Das, A. Das, *Org. Lett.* **2010**, *12*, 3406-3409.

[18] S. Suganya, J. S. Park, S. Velmathi, *J. Fluoresc.* **2016**, *26*, 207-215.

[19] L. Huang, B. Gu, W. Su, P. Yin, H. Li, *RSC Adv.* **2015**, *5*, 76296-76301.

[20] B. A. D. Neto, J. R. Correa, R. G. Silva, *RSC Adv.* **2013**, *3*, 5291-5301.

[21] Z. Xu, L. Xu, *Chem. Commun.* **2016**, *52*, 1094-1119.

[22] A. Pilsl, K. F. Winklhofer, *Acta Neuropathol.* **2012**, *123*, 173-188.

[23] D. M. Krzywanski, D. R. Moellering, J. L. Fetterman, K. J. Dunham-Snary, M. J. Sammy, S. W. Ballinger, *Lab. Invest.* **2011**, *91*, 1122-1135.

[24] D. Nagrath, C. Caneba, T. Karedath, N. Bellance, *Biochim. Biophys. Acta-Bioenerg.* **2011**, *1807*, 650-663.

[25] M. Karbowski, R. J. Youle, *Cell Death Differ.* **2003**, *10*, 870-880.

[26] D. D. Newmeyer, S. Ferguson-Miller, *Cell* **2003**, *112*, 481-490.

[27] D. F. Suen, K. L. Norris, R. J. Youle, *Genes Dev.* **2008**, *22*, 1577-1590.

[28] N. Kumar, V. Bhalla, M. Kumar, *Chem. Commun.* **2015**, *51*, 15614-15628.

[29] J. Bereiter-Hahn, M. Jendrach, In *International Review of Cell and Molecular Biology, Vol 284*; Jeon, K. W., Ed.; Elsevier Academic Press Inc: San Diego, **2010**, *284*, 1-65.

[30] A. T. Hoye, J. E. Davoren, P. Wipf, M. P. Fink, V. E. Kagan, *Acc. Chem. Res.* **2008**, *41*, 87-97.

[31] B. A. D. Neto, P. H. P. R. Carvalho, J. R. Correa, *Acc. Chem. Res.* **2015**, *48*, 1560-1569.

[32] S. T. A. Passos, J. R.Correa, S. L. M. Soares, W. A. da Silva, B. A. D. Neto, *J. Org. Chem.* **2016**, *81*, 2646-2651.

[33] P. H. P. R. Carvalho, J. R. Correa, B. C. Guido, C. C. Gatto, H. C. B. De Oliveira, T. A. Soares, B. A. D. Neto, *Chem. Eur. J.* **2014**, *20*, 15360-15374.

[34] B. A. D. Neto, P. H. P. R. Carvalho, D. C. B. D. Santos, C. C. Gatto, L. M. Ramos, N. M. de Vasconcelos, J. R. Corrêa, M. B. Costa, H. C. B. de Oliveira, R. G. Silva, *RSC Adv.* **2012**, *2*, 1524-1532.

[35] V. V. Rostovtsev, L. G. Green, V. V. Fokin, K. B. Sharpless, *Angew. Chem. Int. Ed*. **2002**, *41*, 2596-2599.

[36] V. F. Ferreira, *Química Nova na Escola* **1996**, *4*, 1-2.

[37] L. F. Fieser, M. Fieser, *J. Am. Chem. Soc.* **1948**, *70*, 3215-3222.

[38] E. N. da Silva Júnior, R. F. S. Menna-Barreto, M. C. F. R. Pinto, R. S. F. Silva, D. V. Teixeia; M. C. B. V. de Souza, C. A. de Simone, S. L. de Castro, V. F. Ferreira, A. V. Pinto, *Eur. J. Med. Chem.* **2008**, *43*, 1774-1780.

[39] F. H. Allen, I. J. Bruno, *Acta Cryst*. **2010**, *B66*, 380-386.

[40] D. Cremer, J. A. Pople, *J. Am. Chem. Soc.* **1975**, *97*, 1354-1358.

[41] B. A. D. Neto, A. S. A. Lopes, G. Ebeling, R. S. Gonçalves, V. E. U. Costa, F. H. Quina, J. Dupont, *Tetrahedron* **2005**, *61*, 10975-10982.

[42] B. A. D. Neto, A. S. Lopes, M. Wüst, V. E. Costa, G. Ebeling, J. Dupont, *Tetrahedron lett.* **2005**, *46*, 6843-6846.

[43] (a) A. V. Pinto, C. N. Pinto, M. C. F. R. Pinto, R. S. Rita, C. Pezzella, S. L. de Castro, *Arzneim-Forsch.* **1997**, *47*, 74-79; (b) C. N. Pinto, A. P. Dantas, K. C. G. Moura, F. S. Emery, P. F. Polaquevitch, M. C. F. R. Pinto, S. L. de Castro, A. V. Pinto, *Arzneim-Forsch*. **2000**, *50*, 1120-1128; (c) K. C. G. Moura, P. F. Carneiro, M. C. F. R. Pinto, J. A. da Silva, V. R. S. Malta, C. A. de Simone, G. G. Dias, G. A. M. Jardim, J. Cantos, T. S. Coelho, P. E. A. da Silva, E. N. da Silva Júnior, *Bioorg. Med. Chem*. **2012**, *20*, 6482-6488.

[44] A. D. Becke, *Phys. Rev. A* **1988**, *38*, 3098-3100.

[45] C. Lee, W.Yang, R. G. Parr, *Phys. Rev. B* **1988**, *37*, 785-789.

[46] S. Grimme, J. Antony, S. Ehrlich, H. Krieg, *J. Chem. Phys.* **2010**, *132*, 154104.

[47] F. Neese, *WIREs: Comput. Mol. Sci.* **2011**, *2*, 73-78.

[48] For aldehyde-bearing dyes see: (a) H. Li, J. Fan, J. Wang, M. Tian, J. Du, S. Sun, P. Sun, X. Peng, *Chem. Commun.* **2009**, 5904-5906. (b) J. Mei, Y. Wang, J. Tong, J. Wang, A. Qin, J. Z. Sun, B. Z. Tang, *Chem. Eur. J.* **2013**, *19*, 613-620. (c) F. Meng, Y. Liu, X. Yu, W. Lin, *New J. Chem.* **2016**, *40*, 7399-7406. (d) W. Wang, O. Rusin, X. Xu, K. K. Kim, J. O. Escobedo, S. O. Fakayode, K. A. Fletcher, M. Lowry, C. M. Schowalter, C. M. Lawrence, F. R. Fronczek, I. M. Warner, R. M. Strongin, J. Am. Chem. Soc. **2005**, *127*, 15949-15958. (e) F. Kong, R. Liu, R. Chu, X. Wang, K. Xu, B. Tang, *Chem. Commun.* **2013**, *49*, 9176-9178. (f) A. Barve, M. Lowry, J. O. Escobedo, K. T. Huynh, L. Hakuna, R. M. Strongin, *Chem. Commun.* **2014**, *50*, 8219-8222. (f) L. Tang, J. Shi, Z. Huang, X. Yan, Q. Zhang, K. Zhong, S. Hou, Y. Bian, *Tetrahedron Lett.* **2016**, *57*, 5227-5231.

[49] D. R. da Rocha, K., I. M. C. B. da Silva, V. F. Ferreira, S. B. Ferreira, F. C. da Silva, *Tetrahedron* **2014**, *70*, 3266-3270.

[50] K. O. Eyong, M. Puppala, P. S. Kumar, M. Lamshöft; G. N. Folefoc, M. Spiteller, S. Baskaran, *Org. Biomol. Chem.*, **2013**, *11*, 459-468.

[51] K. Schaffner-Sabba, K. H. Schmidt-Ruppin, W. Wehrli, A. R. Schuerch, J. W. F. Wasley, *J. Med. Chem.* **1984**, *27*, 990-994.

[52] E. N. da Silva Júnior, R. F. S. Menna-Barreto, M. C. F. R. Pinto, R. S. F. Silva, D. V. Teixeira, M. C. B. V. de Souza, C. A. De Simone, S. L. De Castro, V. F. Ferreira, A. V. Pinto, *Eur. J. Med. Chem.* **2008**, *43*, 1774-1780.

[53] (a) K. C. G. de Moura, K. Salomão, R. F. S. Menna-Barreto, F. S. Emery, M. C. F. R. Pinto, A. V. Pinto, S. L. de Castro, *Eur. J. Med. Chem.* **2004**, *39*, 639-645; (b) K. C. G. de Moura, F. S. Emery, C. N. Pinto, M. C. F. R. Pinto, A. P. Dantas, K. Salomão, S. L. de Castro, A. V. Pinto, *J. Braz. Chem. Soc.* **2001**, *12*, 325-338.

[54] Enraf-Nonius COLLECT; Nonius BV: Delft, The Netherlands, (1997-2000).

[55] Z. Otwinowski, W. Minor, *Methods Enzymol.* **1997**, *276*, 307-326.

[56] Sheldrick, G. M. SHELXS-97. Program for Crystal Structure Resolution. University of Göttingen, Göttingen, Germany, (1997).

[57] G. M. Sheldrick, SHELXL-97. Program for Crystal Structure Refinement. University of Göttingen, Göttingen, Germany, (1997).

[58] L. J. Farrugia, *J. Appl. Crystallogr.* **1997**, *30*, 565-565.

[59] L. J. Farrugia, *J. Appl. Crystallogr.* **1997**, *32*, 837-838.

Entry for the Table of Contents (Please choose one layout)

FULL PAPER

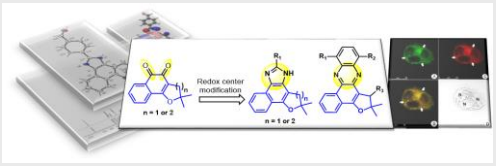

A synthetic strategy for the syntheses of new fluorescent imidazole and phenazine derivatives prepared from naturally occurring naphthoquinones as selective fluorescent mitochondrial imaging probes is reported. These heterocycles presented the same staining patterns of MitoTracker red corroborating the potential of these compounds as new mitochondria markers permeable to the cell membrane.

*Heterocycles and Mitochondrial Imaging Probes

Mitochondrial Heterocyclic Probes*

*Fabíola S. dos Santos et al. and Eufrânio N. da Silva Júnior**

Page No. – Page No.

Redox Center Modification of Lapachones Toward the Syntheses of Nitrogenated Heterocycles as Selective Fluorescent Mitochondrial Imaging Probes